Maryam Eskandari-Nojedehi, Hoda Jafarizadeh-Malmiri* and Javad Rahbar-Shahrouzi

Hydrothermal green synthesis of gold nanoparticles using mushroom (*Agaricus bisporus*) extract: physico-chemical characteristics and antifungal activity studies

DOI 10.1515/gps-2017-0004
Received January 8, 2017; accepted February 13, 2017; previously published online March 23, 2017

Abstract: Edible mushroom (*Agaricus bisporus*) extract was used to synthesize gold nanoparticles (AuNPs) through hydrothermal process (at a pressure of 15 psi and a temperature of 121°C for 15 min). Response surface methodology was applied to monitor the influence of the synthesis parameters, namely: the mushroom extract concentration (1–9 gr DP/100 ml distilled water) and the amount of $HAuCL_4 \cdot 3H_2O$ solution (8–12 ml) on the particle size and concentration of fabricated AuNPs. The obtained results demonstrated that while the main and quadratic terms of the synthesis parameters had significant ($p < 0.05$) effects on the response variables, their interactions had insignificant effect on them. The results indicated that spherical synthesized AuNPs using 10 ml of $HAuCl_4 \cdot 3H_2O$ solution (1 mM) and 1 ml of mushroom extract with concentration of 5 gr DP/100 ml had mean particle size (25 nm) and maximum concentration (534 ppm) and stability (zeta potential of −45.8 mV). The results revealed that mushroom extract could act as both reducing and stabilizing agents due to its bioactive compounds. Fourier-transform infrared analysis showed that polyols and carbonyl groups in mushroom extract had strong effects on formation of stable AuNPs. The fabricated AuNPs exhibited high antifungal activity against *Aspergillus flavus* as compared to the *Aspergillus terreus*.

Keywords: antifungal activity; edible mushroom; gold nanoparticles (AuNPs); green synthesis; hydrothermal process.

***Corresponding author: Hoda Jafarizadeh-Malmiri,** Faculty of Chemical Engineering, Sahand University of Technology, Tabriz 1996-51335, Iran, e-mail: h_jafarizadeh@sut.ac.ir
Maryam Eskandari-Nojedehi and Javad Rahbar-Shahrouzi: Faculty of Chemical Engineering, Sahand University of Technology, Tabriz 1996-51335, Iran

1 Introduction

Metal nanoparticles (NPs) are a source of amazing interest due to their unique properties which in turn, increase their potential applications in several fields. Among other noble metals, gold nanoparticles (AuNPs) due to their optoelectronic properties and biocompatibility find wide application in life sciences [1]. For example, AuNPs are used widely in chemical catalysis, nonlinear optics, surface-enhanced Raman scattering, nanoelectronics, gene expression, disease diagnosis targeted drug delivery, and a controlled release of a drug at the desired site, these days [1–3]. Furthermore, AuNPs have shown high antimicrobial activities against a wide of range of microorganisms, like bacteria and fungi [4, 5]. There are numerous chemical reduction and physical methods which are used in NPs synthesis. However, in all those synthesis methods, the reduction of metal ions occurs using a chemical reducing agent, such as sodium sulfite, hydrazine, and iron (II) sulfate and after the formation of NPs, those stabilize using a chemical stabilizer like polyvinyl pyrrolidone, polyvinyl alcohol, polyaniline, and polyethylene glycol [6–9]. Usage of toxic chemical as reducing and/or stabilizing agents pose potential environmental and biological risks [10]. An environmental-friendly protocol has been proposed for the synthesis of metal NPs without the usage of hazardous chemical, to avoid adverse effects in medical applications [6]. Use of biological systems such as microorganisms (e.g. fungi, bacteria, and yeast) and plant extract or plant biomass could be an alternative to chemical and physical methods for the synthesis of metal NPs such as AuNPs [3, 10].

Edible mushroom is a fleshy fungus and has a spore-bearing fruiting body [11]. Among various mushrooms, *Agaricus bisporus* (button mushroom) is commonly available edible mushroom, revealed to possess wide beneficial properties such as antioxidant, anticancer, antimicrobial [12]. It has been reported that mushroom extracts contain different constituents like terpenoids, tannins, polysaccharide, carbohydrates, phenolic

compounds, and flavonoids which can be applied as a reducing and stabilizing agent in the biosynthesis of NPs [13, 14]. Bhat et al. [7] used edible mushroom *Pleurotus florida* (Oyster mushroom) by photo-irradiation method in the synthesis of AuNPs. They found that triangular- and spherical AuNPs ranged in size from 10 to 50 nm. Sen et al. [15] used glucan of edible mushroom *P. florida* for the synthesis of AuNPs. The synthesis process has been completed by placing in water in 70°C and spherical AuNPs ranging from 70 to 500 nm in size were formed.

Chemical reduction of metal ions using a chemical reducing agent can be carried out at room temperature. But in bioreduction of the ions using the microorganism and plant extracts, due to low concentration of the bioreductants, the temperatures of synthesis process should be elevated for a higher reaction rate. Recently it has been demonstrated that thermal factor affects the size and uniformity of the formed NPs [16]. Hydrothermal synthesis of AuNPs by autoclave is one of the practical synthesis method because the system is capable of simultaneously generating high pressure and high temperature. Reddy et al. [17] used gum *Kondagogu* by autoclave for the synthesis of AuNPs. They synthesized spherical AuNPs with a particle size of 12 ± 2 nm.

To the best of our knowledge, there are no reports on green synthesis of AuNPs using hydrothermal method and mushroom extract. However, there are a few reports on antifungal activity of AuNPs. Therefore, the main objectives of the present study were: (i) to hydrothermally green synthesize AuNPs using mushroom extract; (ii) to optimize the AuNPs synthesis process; and (iii) to evaluate physico-chemical properties and antifungal activity of the fabricated AuNPs against *Aspergillus flavus* and *Aspergillus terreus*.

2 Materials and methods

2.1 Materials

Fresh edible mushrooms *A. bisporus*, same in shape and size, were obtained from local market in Tabriz, Iran. Gold (III) chloride trihydrate ($HAuCl_4 \cdot 3H_2O$) as gold ions precursors and AuNPs standard solution (with particle size of 10 nm and concentration of 100 ppm) were purchased from Sigma-Aldrich (Sigma-Aldrich co. MO, USA) and Tecnan-Nanomat (Tecnan-Nanomat co, Navarra, Spain), respectively. *Aspergillus flavus* (PTCC 5004) and *A. terreus* (PTCC 5021) were provided by microbial Persian type culture collection (PTCC, Tehran, Iran). Potato dextrose agar (PDA) as culture media was purchased from Oxoid (Oxoid Ltd., Hampshire, England). All aqueous solutions were prepared by using freshly double distilled water.

2.2 Preparation of aqueous mushroom extract

The mushrooms were washed repeatedly with double distilled water to remove organic impurities present on their surface, crushed into small pieces, and then shade dried for 3 days. The dried mushroom pieces were powdered using domestic miller (MX-GX1521, Panasonic, Tokyo, Japan). The broth used for the reduction of Au^{3+} ions to Au^0 was prepared by taking 5 g of the mushroom powdered in 250 ml Erlenmeyer flasks with 100 ml of double distilled water and then boiled for 10 min, and filtrated through Whatman No. 1 filter paper. The provided mushroom extract was stored in the refrigerator at 4°C until further use.

2.3 Synthesis of AuNPs using mushroom extract

Gold (III) chloride trihydrate (1 mM) solution was prepared by dissolving 0.392 g of its powder in 100 ml of double distilled water. Different amounts of 1 mM gold ions precursors solution (8–12 ml) were mixed with 1 ml of mushroom extract with different concentrations ranging from 1 to 9 g of mushroom dried powder/100 ml of distilled water (gr DP/100 ml) in boiling tubes and then kept in autoclave at pressure of 15 psi and temperature of 121°C for 15 min.

2.4 Analysis

2.4.1 Mushroom extract characteristics: In order to identify the reducing and stabilizing biomolecules in *A. bisporus* (white button mushroom) extract which were effective in AuNPs synthesis, FT-IR measurements were carried out. The FT-IR spectra of mushroom extract were recorded on a Bruker Tensor 27 spectrometer (Bruker, Germany) using KBr pellets in the 4000–400 cm^{-1} region [18]. The pH measurement of mushroom extract solution was performed by pH meter (DELTA 320, Shanghai, China). Generally, the size, shape, and yield of NPs synthesis are mainly affected by the change in a charge in the natural phytochemicals existing in an extract as their capability to bind and reduce metal captions [19].

2.4.2 Physico-chemical characteristics of the synthesized AuNPs: The formation of AuNPs was confirmed by using UV-visible spectroscopy due to the presence of a localized surface plasmon resonance signal (SPR) in the visible part of the spectrum, using a Jenway UV-Vis spectrophotometer 6705 (UK) in a 1 cm optical path quartz cuvette. The absorbance is proportionate to the concentration of synthesized AuNPs. It can be calculated using a standard curve which was established by several serial dilution solutions of the standard AuNPs solution (10–100 ppm).

A dynamic light scattering particle size analyzer (Nanotrac Wave, Microtrac, USA) was used to estimate the values of mean particle size, polydispersity index (PDI), and zeta potential of the synthesized AuNPs at 25°C.

X-ray diffraction (XRD) study was carried out using the films of colloidal synthesized AuNPs formed on a microscopic glass slide by drop coating to confirm the crystallinity. The XRD analysis of the AuNPs was performed using Siemens D5000 diffractometer (Tokyu, Japan) with Cu-Kα radiation ($\lambda = 1.54178$ Å). The device operated at 35 kV and 2θ diffraction angles ranged from 30° to 90°.

The morphology of the synthesized AuNPs was observed by transmission electron microscopy (TEM, CM120, Philips, Amsterdam, Netherlands) with an acceleration voltage of 120 kV.

2.4.3 Antifungal activity of the synthesized AuNPs: The antifungal activity of the synthesized AuNPs against *A. flavus* and *A. terreus* was assessed according to the method described by Mohammadlou et al. [20]. In fact, the inhibition in radial mycelia growth of *A. flavus* and *A. terreus* on the plates (90 ml in diameter) containing of PDA incorporated with AuNPs was evaluated during 7 days and antifungal activity of AuNPs was expressed as fungal hyphae growth (mm).

2.5 Design of experiments and statistical analysis

Central composite design with two independent variables, namely: mushroom extract concentration or MEC (1–9 g/100 ml) (X_1) and amount of 1 mM $HAuCl_4$ solution (8–12 ml) (X_2), was used to design experiments using the software Minitab v.16 statistical package (Minitab Inc., PA, USA). Response variables were chosen according to the literature [20]. Response surface methodology due to its ability to generate large amounts of information from a small number of experiments and the possibility of evaluating the interaction effect between the variables on the responses [λ_{max} (Y_1) and AuNPs concentration (Y_2)], was applied to assess the relationships between the studied responses and synthesis variables and to optimize them in order to gain the desired characteristics of the product (the least λ_{max} and the highest AuNPs concentration) [21]. All experiments (13 runs) were carried out in 1 day (one block) and at five different levels, including four factorial points, four star points, and five center points using the software Minitab v.16 statistical package (Minitab Inc., PA, USA) (Table 1). Five replicates were performed at a central point for estimation of the pure error [22]. A second-order polynomial equation (Eq. 1) was used to express the response variables (Y_i) of the synthesized AuNPs as a function of the studied synthesis variables (X_i).

$$Y_i = \beta_0 + \sum \beta_i X_i + \sum \beta_{ii} X_i^2 + \beta_{ij} X_i X_j \quad (1)$$

where Y_i is the response variable, β_0, β_i, β_{ii}, and β_{ij} represent the constant, linear, quadratic and interaction terms, respectively. The adequacy of model was examined accounting for the coefficient of determination (R^2) and adjusted the coefficient of determination (R^2-adj). To fit the second-order polynomial equation, analysis of variance was used to analyze the experimental data by multiple linear regressions, and the statistical significance of each regression term was evaluated using the p-value from the pure error obtained from replicates at the central point. The p-values lower than 0.05 were considered to be statistically significant. For the graphical analysis of the independent variable, two-dimension contour plots were obtained from the fitted polynomial [23]. It should be noted that the presented correlation is valid only within the range of variables investigated. Graphical and numerical multiple response optimizations were used to determine the optimum levels of MEC and amount of $HAuCl_4$ to attain the desired response goals [minimum value for λ_{max} (AuNPs size) as well as a maximum value of AuNPs concentration] [24]. Subsequently, three additional confirmation experiments were conducted to verify the validity of the statistical experimental strategies.

Table 1: Central composite design and response variables (experimental and predicted value) for synthesis of gold nanoparticles using mushroom extract.

Sample no.	MEC (gr DP/100 ml)	Amount of $HAuCl_4$ (ml)	λ_{max} (nm)		Concentration (ppm)	
			Exp[a]	Pre[b]	Exp[a]	Pre[b]
1	5.0	10.0	551	551	513	534
2	5.0	12.0	544	544	516	509
3	2.2	8.6	552	553	312	273
4	5.0	10.0	550	550	554	534
5	5.0	10.0	550	550	539	540
6	1.0	10.0	553	552	84	130
7	5.0	8.0	550	548	457	468
8	2.2	11.4	550	549	295	268
9	7.8	8.6	537	539	479	502
10	9.0	10.0	535	533	545	503
11	5.0	10.0	550	552	531	534
12	5.0	10.0	552	547	535	538
13	7.8	11.4	536	536	531	567

[a]Experimental values of studied responses.
[b]Predicted values of studied responses.

3 Results and discussion

3.1 Mushroom extract characteristics

The FT-IR images of the mushroom extract and extract containing AuNPs samples show a number of functional bonds associated with them which provide them with stability by capping them. As clearly observed in Figure 1, it can be inferred that the samples have four main peaks in the range of 1107.57, 1421.22, 1637.72, and 3446.58 cm^{-1} and two weak peaks at wavenumbers of the 569.59 and 2934.08 cm^{-1}. The broad peak obtained in the range of 3100–3600 cm^{-1} corresponds to the O–H and N–H bond stretching vibrations. A minor peak at around 2934.08 cm^{-1} suggests the presence of carboxylic and phenolic compounds. The peak at 1637.72 cm^{-1} corresponding to amide I due to carbonyl stretch and –N–H stretch vibrations in the amide linkages of the protein correspondingly. The band at 1421.22 cm^{-1} is the C–N stretching mode of aromatic amine group. The C–O–C and C–OH vibrations of the protein/polysaccharide in the mushroom extract appear as a medium IR band at 1107.57 cm^{-1}. These peaks ranging from 1107.57 to 1637.72 cm^{-1} also observed in IR band of mushroom extract including AuNPs which confirmed that the carbonyl group of amino acid residue and peptides of proteins have strong ability to bind metal, and so the proteins most possibly might have formed a layer on the AuNPs and also prevented agglomeration of the particles,

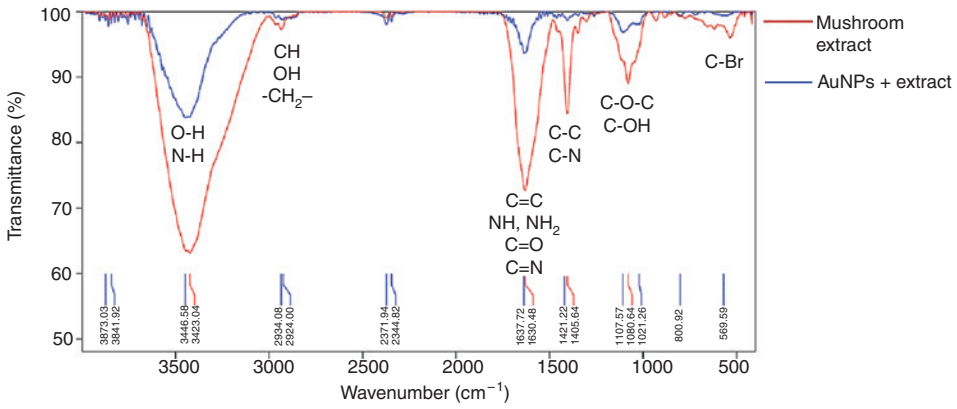

Figure 1: FT-IR spectrum of mushroom extract and mushroom extract containing AuNPs.

and thus the NPs are stabilized in the medium [7]. Mushrooms are rich in proteins and have high amount of amino acids such as lysine, tryptophan, glutamic acid, and aspartic acid [25]. Adsorption peaks around 569.59 cm^{-1} are attributed to R–CH groups. The obtained results were in agreement with the findings of Narasimha et al. [26] and Eskandari et al. [22]. They found the FT-IR spectrum for *A. bisporus* between 500 and 4000 cm^{-1}, which confirmed the presence of proteins, carbonyl groups, esters, and carboxylic acids for the synthesis and stabilization of silver and gold NPs. The mean pH value of mushroom extract was about 6.25 ± 0.20 which represents that mushroom extract, due to its high amount of phenolic acid (Figure 1), is an acidic media.

3.2 Fitting the response surface models

The responses obtained from the experimental runs, which are shown in Table 1, were fitted to second-order polynomial models by applying multiple regression analysis for studying two synthesis parameters. Therefore, the estimated regression coefficients, either for initial or final reduced models, as well as the corresponding significance of regressions are given in Table 2.

The F-ratio and p-value of each term in suggested models, which provides their significance determinations, are also shown in Table 3. It should be considered that in significance determination of terms, lower p-value and higher F-ratio correspond to a higher significance of a term on studied response variations. The obtained final models were valid only in the studied independent variable levels [27, 28].

As the coefficients of determinations (R^2 and adjusted R^2) are good measure for overall model performance, their obtained relatively high values confirmed the suitability of suggested models. Furthermore, attained insignificant lack of fits for suggested models ensured their adequate fitness to the independent variable effects (Table 2). As

Table 2: Regression coefficients, R^2, adjusted R^2 (R^2-adj), and probability values for the final reduced models suggested for synthesis of AuNPs.

Regression coefficient	λ_{max} (nm)	Concentration (ppm)
β_0 (constant)	380.124	−1559.06
β_1 (main effect)	1.718	146.42
β_2 (main effect)	34.970	315.62
β_{11} (quadratic effect)	−0.412	−10.72
β_{22} (quadratic effect)	−1.775	−15.26
β_{12} (interaction effect)	–[a]	–[a]
R^2	99%	94.72%
R^2-adj	98.34%	91.70%
Lack of fit	1.14	5.63
p value (regression)	0.406	0.064

β_0 is a constant; β_i, β_{ii}, and β_{ij} are the linear, quadratic, and interaction coefficients of the quadratic polynomial equation, respectively.
1, mushroom extract (gr DP); 2, $HAuCl_4$ (ml).
[a]Is zero due to nonsignificance of its interaction.

Table 3: The significance probability (p-value and F-ratio) of regression coefficients for the final reduced models suggested for AuNPs synthesis.

Main effects	Main effects		Quadratic effects		Interacted effects
	X_1	X_2	X_1^2	X_2^2	X_1X_2
λ_{max} (Y_1, nm)					
p-Value	0.013	0.001	0.000	0.001	–[a]
F-ratio	12.21	34.29	74.37	35.44	–[a]
Concentration (Y_2, ppm)					
p-Value	0.000	0.016	0.000	0.019	–[a]
F-ratio	69.18	9.87	47.72	9.26	–[a]

1, mushroom extract (gr DP); 2, $HAuCl_4$ (ml).
[a]Not significant ($p > 0.05$).

shown in Table 3, the linear and quadratic effects of the synthesis parameters had significant ($p < 0.05$) effects on all studied characteristics of formed NPs. The resulted regression coefficients and their p-values and F-ratios revealed that, however, the positive signs of the main effect of provided complicated variation of these response with studied synthesis parameters, but the negative sign of the quadratic regression coefficients presented the generally inverse changes of AuNPs concentration and λ_{max} by both MEC and amount of $HAuCl_4$ (Table 2).

3.2.1 Maximum wavelength (λ_{max})

The change in color of the reaction mixture including mushroom extract and $HAuCl_4$ from colorless to pinkish violet colored was observed in Figure 2. This color arises due to excitation of surface Plasmon vibrations in metal NPs and confirmed by UV-visible spectroscopy [29, 30]. The UV-visible spectroscopy is also a very useful technique which allows estimating of the size and concentration of synthesized AuNPs in the colloidal solution. The AuNPs exhibit an intense absorption peak (λ_{max}) that ranged from 510 to 570 nm due to SPR. In fact, the particle size of the formed NPs can be manifested in the λ_{max} of the NPs. It is well known that the longer wavelengths in absorption spectra of metal NPs are correlated to their bigger size [20, 31]. Figure 2 shows the UV-visible spectra of the synthesized AuNPs sample. The λ_{max} of the synthesized AuNPs ranged from 535 to 552 nm (Table 1). In all cases, λ_{max} was obtained in favorable range for AuNPs in UV-visible analysis. The λ_{max} can be correlated to the particle size of the formed NPs as the longer wavelengths correspond to increase in particle size [32]. The effects of MEC and amount of $HAuCl_4$ solution on the AuNPs size changes (λ_{max}) are shown in Figure 3A and B. As clearly observed in Figure 3A, at constant amount of $HAuCl_4$, by increasing the MEC, the size of AuNPs decreased. The result can be explained by the fact that at high MEC, the amount of

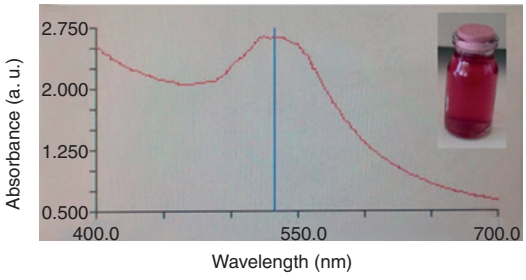

Figure 2: A UV-Vis spectra sample of the mixture solution containing $HAuCl_4$ and mushroom extract, after synthesis of AuNPs.

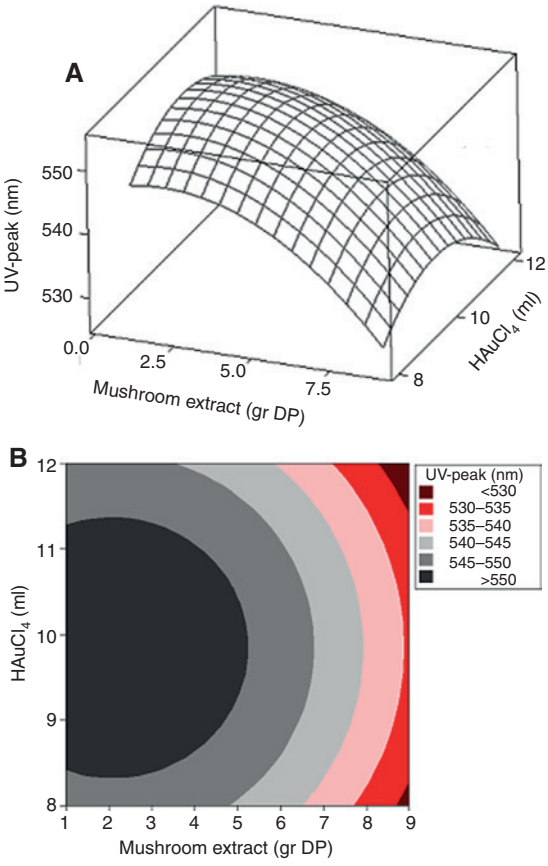

Figure 3: Surface plot (A) and contour plot (B) for λ_{max} of the synthesized AuNPs as function of MEC (g/100 ml) and the amount of $HAuCl_4$ (ml).

reducing agents is high which in turn, can rapidly reduce Au ions and form AuNPs. On the other hand, due to the high concentration of stabilizing agents in the extract, the carbonyl group of proteins (band at 1637.84 cm^{-1} at Figure 1) form a covering layer on the formed AuNPs and act as stabilizing agent to prevent their agglomeration [33]. As clearly observed in Figure 3B the minimum λ_{max} (535 nm) could be achieved at high amount of $HAuCl_4$ solution and high MEC. The obtained results were in agreement with finding of Sadeghi et al. [34]. They found the carbonyl group of proteins in *Stevia rebaudiana* leaf extract adsorbed strongly to metals and it could have formed a layer along with the bio-organics, securing interaction with biosynthesized AuNPs. As clearly observed in Figure 3B, at a mean amount of $HAuCl_4$, by decreasing the MEC, the size of AuNPs increased. The result shows that low concentration of both reducing and stabilizing agents of low MEC, a few Au ions turn to AuNPs and due to low concentration of stabilizing agents, the formed AuNPs rapidly agglomerated and their particle size increased [35]. The obtained result was in agreement with the findings of

Dwivedi and Gopal [35]. They indicated that at high concentration of $HAuCl_4$, at constant *Chenopodium album* leaf extract concentration, the surface Plasmon peak minor red-shift decreased in the intensity of the peak.

3.2.2 Concentration of AuNPs

As clearly observed in Table 2, by increasing both MEC and amount of $HAuCl_4$ at low levels, the AuNPs concentration increased, at lower levels of those independent variables, the concentration of the synthesized AuNPs decreased. As clearly observed in Table 3, the MEC affected the AuNPs concentration more significantly as compared to amount of $HAuCl_4$. Therefore, MEC is considered to be the most vital parameter in the determination of this response. As shown in Figure 4A, at low and high amounts of $HAuCl_4$, by decreasing the amount of MEC the concentration of AuNPs solution decreased. The obtained result was in agreement with findings of Dwivedi and Gopal [35]. They indicated that at high concentration of *Chenopodium album* leaf extract at constant Au ions concentration, the absorbance peak of NPs solution was increased, therefore, the concentration of AuNPs colloids was increased. The obtained results indicated that the minimum concentration was obtained at minimum MEC and maximum amount of $HAuCl_4$ (295 ppm) and maximum concentration was formed at central range of MEC and amount of $HAuCl_4$ (554.04) (Figure 4B).

3.3 Optimization of processing parameters for the synthesized AuNPs

The AuNPs would be considered an optimum product if the process resulted in the smallest mean particle size (λ_{max}) and highest AuNPs concentration. Therefore, an overlaid contour plot as a graphical optimization approach was used to find the optimum region for synthesis variables in order to synthesize AuNPs with the minimum λ_{max} and maximum AuNPs concentration (Figure 5). The specified white colored area in Figure 5 indicated the desired MEC and amount of $HAuCl_4$ levels to get the optimum AuNPs products. Numerical multiple optimization was also used to find the exact optimum levels of studied synthesis variables. The results also showed that the synthesis conditions with a $HAuCl_4$ of 10 ml for 5 g MEC in preparation of AuNPs would give the most desirable products with λ_{max} in 550 nm wavelength and the synthesized AuNPs with concentration of 534 ppm. Moreover, three AuNPs solutions were prepared according to the recommended optimal levels by numerical multiple optimization and characterized in terms of studied physicochemical properties. The mean measured experimental values for the λ_{max} and AuNPs

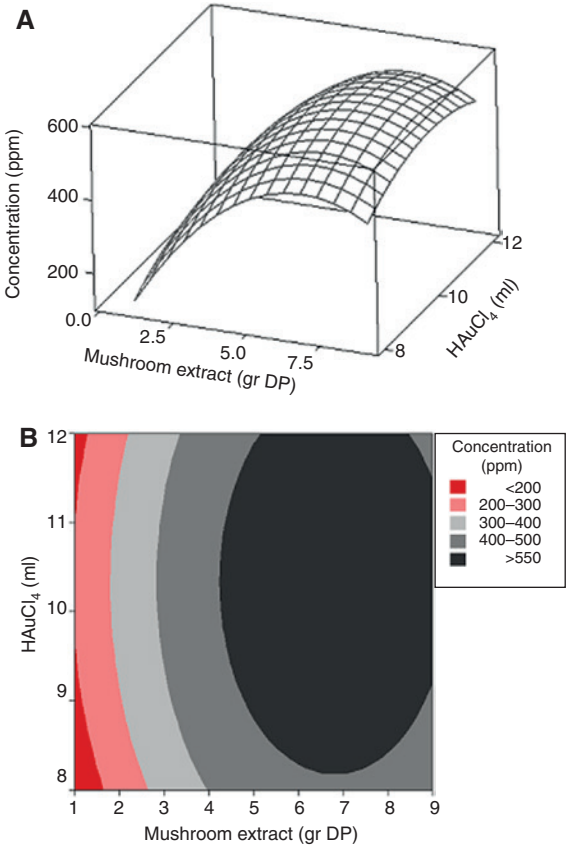

Figure 4: Surface plot (A) and contour plot (B) for concentration of synthesized AuNPs as function of MEC (g/100 ml) and amount of $HAuCl_4$ (ml).

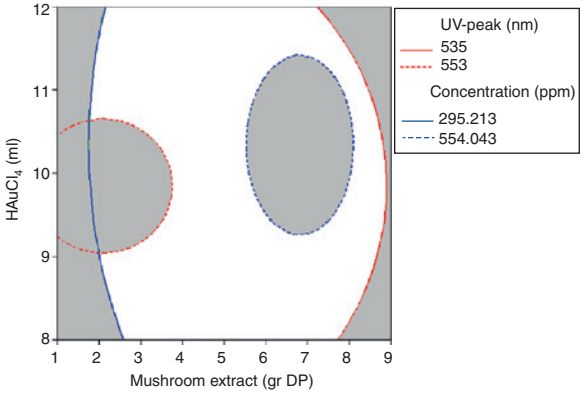

Figure 5: Overlaid contour plot of AuNPs λ_{max} and concentration with acceptable levels as function of MEC (g/100 ml) and amount of $HAuCl_4$ (ml).

concentration of these three AuNPs solution samples were 551 ± 1 nm and 535.54 ± 1.16 ppm, respectively. The overall similarities between the experimental and predicted values for these characteristics established the adequacy of the suggested regression equations.

3.4 Physico-chemical characteristics of the synthesized AuNPs at optimum synthesis conditions

The particle size, PDI, and zeta potential values and concentration of the synthesized AuNPs at optimum synthesis conditions were 32.1 nm, 0.597, −45.8 mV and 534 ppm, respectively. The dynamic light scattering technique involves scattering of a laser light beam at the surface of dispersed NPs and detection of the backscattered light. PDI is a dimensionless approximation that describes the homogeneity of NPs. Its value changes from 0 to 1, and smaller values correspond to a narrower and finer particle size distribution [21]. It is more desirable to get AuNPs with lower PDI. Zeta potential measurements reveal the NPs are highly stable and have an average surface charge of −45.8 mV. The higher zeta-potential value is a key parameter to maintain the stability of suspension through the electrostatic repulsion between particles, which results in a high stability of suspension. Solutions with zeta potential above +20 mV or below −20 mV are considered stable [36]. The obtained results were in agreement with finding of Chen et al. [37]. They found the zeta potential of synthesis AuNPs was −16.6 at 0.33 mg/ml bromelain extract for the biosynthesis of AuNPs using bromelain.

The size distribution of NPs leads to inhomogeneous broadening of the resonance due to the variation in the resonant energy level [38]. The peak intensity and full width at half maximum depends on size and extent of aggregation of particles and the broadness of the peak attributes to the broad particle size distribution [39]. The size distribution of the synthesized AuNPs obtained at optimum conditions was also shown in Figure 6. As clearly can be seen in these figures, the size distribution of the formed AuNPs is monomodal. The monomodal size distributions was favored compared to polymodal distributions, because the polymodal particle distributions can speed up the Oswald ripening of particles and decrease the physical stability of the NPs solutions.

The crystalline nature of AuNPs was confirmed from the XRD analysis. Figure 7 shows the XRD pattern of synthesized AuNPs using mushroom extract. The diffraction peaks at 38.1°, 44.5°, 64.6°, and 77.8° correspond

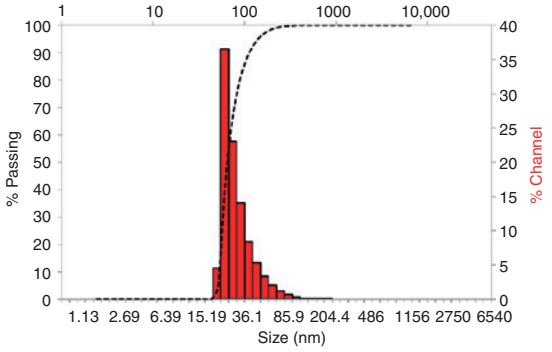

Figure 6: Particle size distribution of synthesized AuNPs at obtained optimum synthesis conditions.

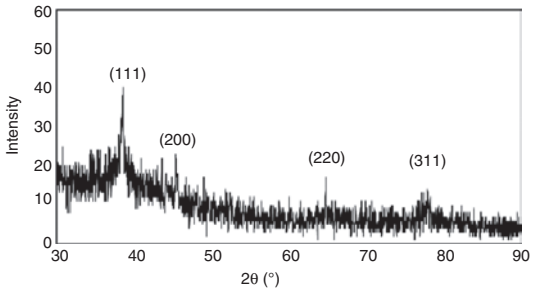

Figure 7: X-ray diffraction pattern of the synthesized AuNPs using mushroom extract at obtained optimum conditions.

to the (111), (200), (220), and (311) planes of face centered cubic (fcc) crystal structure, respectively [15, 25]. However, according to Figure 7 the aforementioned peaks are not very sharp and it indicates that the synthesized AuNPs using mushroom extract have not got crystallinity.

Transmission electron microscopy (TEM) has been used to identify the size, shape, and morphology of NPs. Typical TEM images obtained from the final optimized AuNPs colloid are shown in Figure 8. A typical TEM image of biologically synthesized AuNPs, indicated that the synthesized AuNPs were well dispersed with spherical structure and particle sizes ranging from 10 to 50 nm, and a mean particle size of 25 nm. The obtained results were in agreement with findings of Bhat et al. [7]. They found the diameter of synthesis AuNPs was ranging from 10 to 50 nm and the morphology of the NPs was spherical for the photo-biosynthesis of AuNPs using edible mushroom *Pleurotus florida*.

The results of our previous research, related to the green synthesis of AuNPs using mushroom extract and microwave technique, indicated that the well-dispersed and spherical AuNPs with the minimum mean particle size and PDI, and maximum concentration and zeta

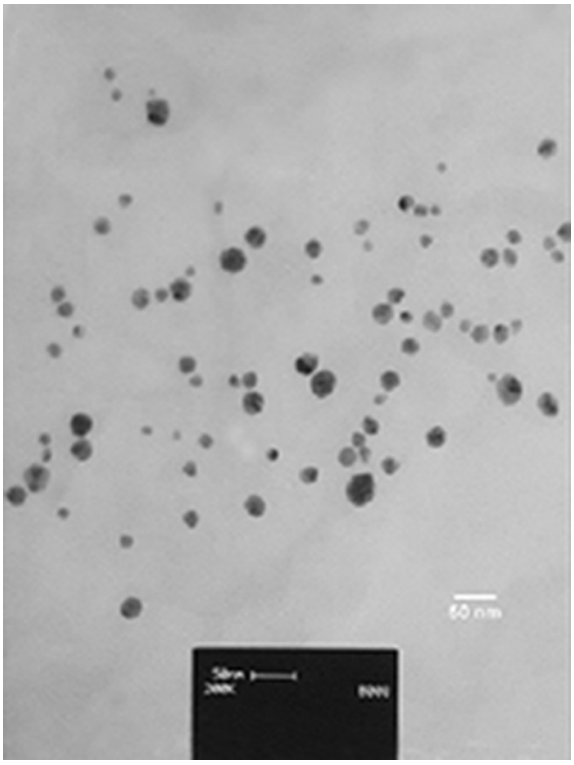

Figure 8: TEM image of the synthesized AuNPs using mushroom extract at obtained optimum conditions.

potential of the 33.56 nm, 0.855 ppm, 148.88 ppm, and +17.2 mV, respectively, were obtained using 2.62 ml of $HAuCl_4$ and 0.2 ml of mushroom extract during microwave exposure time of 55 s [22]. The results of the present study indicated that as compared to microwave synthesis method, the hydrothermal AuNPs synthesis technique, could result in fabrication of the AuNPs with smallest mean particle size and highest stability (zeta potential value). This can be explained by the fact that by increasing the NPs synthesis time and the temperature of the colloidal solution, rate of the nucleation and growth of the NPs increase and after that, it increases NPs collision rate, which in turn decreases the particle size of the synthesized NPs [20].

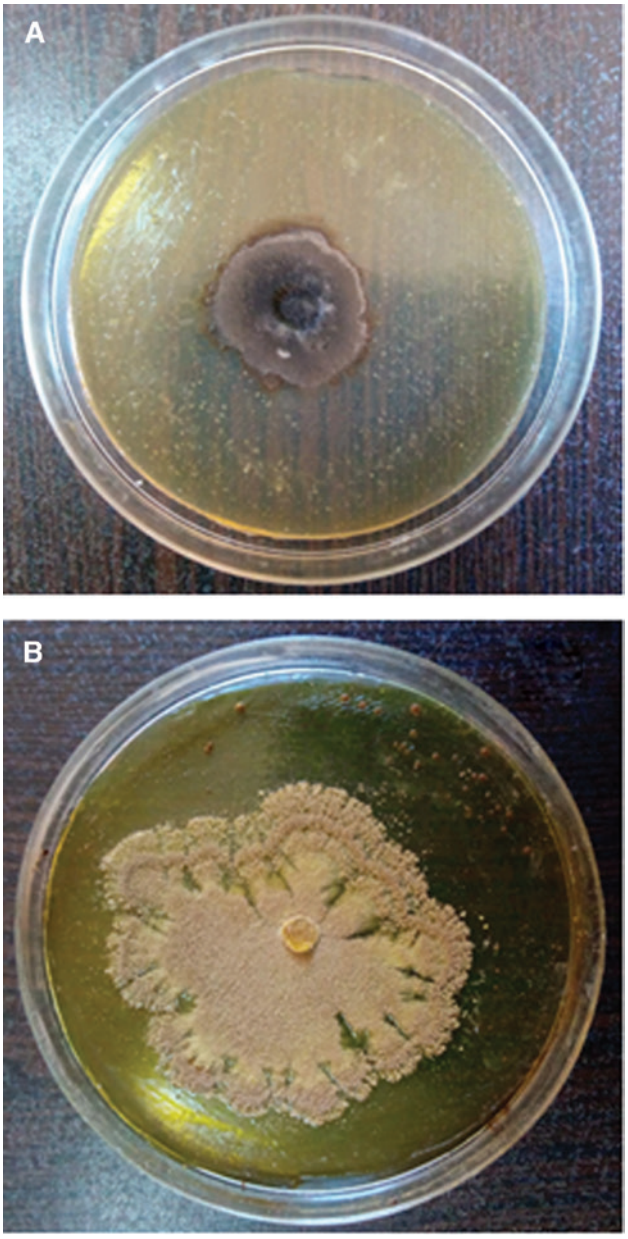

Figure 9: Mycelia growth inhibition of the synthesized AuNPs toward A. flavus (A) and A. terreus (B) after 10 days of incubation at 26°C ± 2°C.

3.5 Antifungal activity of AuNPs

Effects of synthesized AuNPs on mycelia growth of *A. flavus* and *A. terreus* during 10-day incubation period are shown in Figure 9A and B, respectively. As clearly observed in these figures, AuNPs amended in PDA media could inhibit the mycelia growth of *A. flavus*. As clearly observed in Figure 10A, AuNPs conjugated with PDA medium culture had significant fungicidal effect on *A. flavus*. While, the synthesized AuNPs showed low fungicidal effect on *A. terreus* (Figure 10B). The obtained result was in line with findings of Eid et al. [40]. They indicated that *Pencillium* growths were completely inhibited upon treatment with 130 μM of AuNPs solution. It has been generally believed that the mechanism of the antifungal effects of gold ions involves their absorption and accumulation by the fungus cell that would lead to shrinkage of the cytoplasm membrane or its detachment from the cell wall.

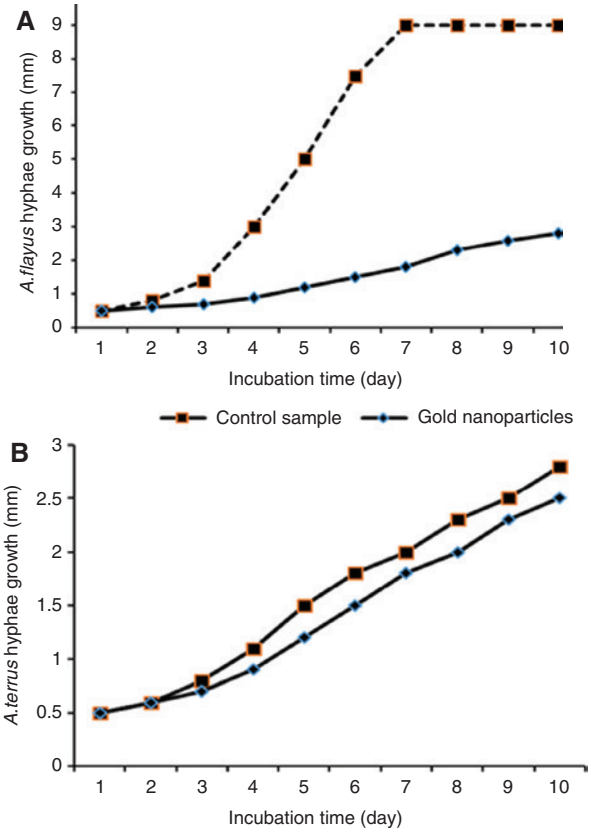

Figure 10: Antifungal effects of the synthesized AuNPs obtained at optimum conditions on A. flavus (A) and A. terreus (B). Data are the mean value of three replicates (each replicate contains four plates).

4 Conclusions

Green synthesis of AuNPs using hydrothermal technique and edible mushroom (*A. bisporus*) extract as reducing and capping agents, was carried out in the present study. This novel synthesis route provides a simple, efficient, environmental friendly and low cost method, as compared to currently available chemical and/or physical NPs synthesis methods. The results indicated the usefulness of response surface methodology for studying the effects of the synthesis conditions on the dependent variables and to optimize them in order to get the most desirable AuNPs. These green synthesized AuNPs had also suitable fungicidal effect against to *A. flavus* and *A. terreus*.

Acknowledgments: The authors would like to acknowledge the Iran Nanotechnology Initiatives Council (INIC) for funding the development of an innovative methodology for safety assessment of industrial nanomaterials (grant no. 84465).

References

[1] Yue H-L, Hu Y-J, Chen J, Bai A-M, Ouyang Y. *Colloids Surf. B Biointerfaces* 2014, 122, 107–114.
[2] Abdelhalim MAK, Mady MM, Ghannam MM. *J. Nanomed. Nanotechol.* 2012, 3, 133–138.
[3] Aromal SA, Philip D. *Spectrochim. Acta Mol. Biomol. Spectrosc.* 2012, 97, 1–5.
[4] Ahmad T, Wani IA, Lone IH, Ganguly A, Manzoor N, Ahmad A, Ahmed J, Al-Shiri AS. *Mater. Res. Bull.* 2013, 48, 12–20.
[5] Wani IA, Ahmad T. *Colloids Surf. B Biointerfaces* 2013, 101, 162–170.
[6] Kanchi S, Kumar G, Lo A-Y, Tseng C-M, Chen S-K, Lin C-Y, Chin T-S. *Arabian J. Chem.* doi:10.1016/j.arabjc.2014.08.006.
[7] Bhat R, Sharanabasava V, Deshpande R, Shetti U, Sanjeev G, Venkataraman A. *J. Photochem. Photobiol. B.* 2013, 125, 63–69.
[8] Kharissova OV, Dias HR, Kharisov BI, Pérez BO, Pérez VMJ. *Trends Biotechnol.* 2013, 31, 240–248.
[9] Su C-H, Wu P-L, Yeh C-S. *J. Phys. Chem. B.* 2003, 107, 14240–14243.
[10] Sankar R, Karthik A, Prabu A, Karthik S, Shivashangari KS, Ravikumar V. *Colloids Surf. B.* 2013, 108, 80–84.
[11] Ifuku S, Nomura R, Morimoto M, Saimoto H. *Materials* 2011, 4, 1417–1425.
[12] Mirunalini S, Arulmozhi V, Deepalakshmi K, Krishnaveni M. *Not. Sci. Biol.* 2012, 4, 55–61.
[13] Gan C, Nurul Amira B, Asmah R. *Int. Food Res. J.* 2013, 20, 1095–1102.
[14] Rao JS, Kumar KR, Vale VK, Yarlagadda PP, Saradhi SV. *J. Chem. Biol. Phys. Sci.* 2013, 3, 1222–1228.
[15] Sen IK, Maity K, Islam SS. *Carbohyd. Polym.* 2013, 91, 518–528.
[16] Singh PP, Bhakat C. *Chem. Mater. Res.* 2012, 2, 82–87.
[17] Reddy GB, Madhusudhan A, Ramakrishna D, Ayodhya D, Venkatesham M, Veerabhadram G. *J. Nanostruct. Chem.* 2015, 5, 185–193.
[18] Wilberley S, Sprague JW, Campbell *J. Anal. Chem.* 1957, 29, 210–213.
[19] Makarov V, Love A, Sinitsyna O, Makarova S, Yaminsky I, Taliansky M, Kalinina NO. *Acta Naturae* 2014, 6, 35–44.
[20] Mohammadlou M, Jafarizadeh-Malmiri H, Maghsoudi H. *Green Process. Synth.* 2017, 6, 31–42.
[21] Anarjan N, Jafarizadeh-Malmiri H, Nehdi IA, Sbihi HM, Al-Resayes SI, Tan CP. *Int. J. Nanomed.* 2015, 10, 1109–1118.
[22] Eskandari M, Jafarizadeh-Malmiri H, Rahbar-Shahrouzi J. *Nanotechnol. Rev.* 2016, 5, 537–548.
[23] Gharibzahedi SMT, Mousavi SM, Hamedi M, Khodaiyan F, Razavi SH. *Carbohyd. Polym.* 2012, 87, 1611–1619.
[24] Anarjan N, Mirhosseini H, Baharin BS, Tan CP. *Food Chem.* 2010, 123, 477–483.
[25] Philip D. *Spectrochim. Acta Mol. Biomol. Spectros.* 2009, 73, 374–381.
[26] Narasimha G, Praveen B, Mallikarjuna K, Deva Prasad Raju B. *Int. J. Nano Dimens.* 2011, 2, 29–36.
[27] Anarjan N, Jaberi N, Yeganeh-Zare S, Banafshehchin E, Rahimirad A, Jafarizadeh-Malmiri H. *J. Am. Oil Chem. Soc.* 2014, 91, 1397–1405.
[28] Jafarizadeh-Malmiri H, Osman A, Tan CP, Abdul Rahman R. *J. Food Process. Preserv.* 2012, 36, 252–261.

[29] Bulavchenko A, Arymbaeva A, Tatarchuk V. *Russ. J. Phys. Chem. A* 2008, 82, 801–806.
[30] Thanh NT, Maclean N, Mahiddine S. *Chem. Rev.* 2014, 114, 7610–7630.
[31] Chanda S. In *Microbial pathogens and strategies for combating them: science, technology and education*, Mendez-Vilas A, Ed., Formatex Research Center: Badajoz, Spain. 2014, pp. 1314–1323.
[32] Stalmashonak A, Seifert G, Abdolvand A. In *Ultra-short pulsed laser engineered metal-glass nanocomposites*. Springer: New York, 2013, pp. 5–15.
[33] Medda S, Hajra A, Dey U, Bose P, Mondal NK. *Appl. Nanosci.* 2015, 5, 875–880.
[34] Sadeghi B, Mohammadzadeh M, Babakhani B. *J. Photochem. Photobiol. B* 2015, 148, 101–106.
[35] Dwivedi AD, Gopal K. *Colloids Surf. A.* 2010, 369, 27–33.
[36] Eastman J. In *Colloid science: Principles, methods and applications*, Cosgrove T, Ed., Blackwell Publishing Ltd.: UK, 2005, pp. 36–49.
[37] Chen Z, Mochizuki D, Wada Y. In *Microwaves in nanoparticle synthesis: fundamentals and applications*, Horikoshi S, Serpone N, Eds., John Wiley & Sons: Germany, 2013, pp. 145–180.
[38] Bahk J-H, Shakouri A. In *Nanoscale thermoelectrics*, Wang X, Wang ZM, Wang XS, Eds., Springer: New York, 2014, pp. 41–92.
[39] Sharma A, Dhiman N, Singh BP, Gathania AK. *Mater. Res. Express*. 2014, 1, 025042.
[40] Eid KA, Salem HF, Zikry AA, El-Sayed AF, Sharaf MA. *Nat. Sci. Sleep* 2011, 29, 29–33.

Bionotes

Maryam Eskandari-Nojedehi

Maryam Eskandari-Nojedehi obtained her BSc degree in food engineering (applications of carboxymethyl cellulose in food products) in 2012. She obtained her MSc degree in chemical engineering with major on food engineering from Sahand University of Technology, Iran (2015). The present study is the result of her Master's thesis (supervisors: Assis. Prof. Hoda Jafarizadeh-Malmiri and Javad Rahbar-Shahrouzi). Her field of interest is green synthesis of metal nanoparticles and evaluation of their antimicrobial activity.

Hoda Jafarizadeh-Malmiri

Hoda Jafarizadeh-Malmiri received his BSc and MSc degrees in food engineering (Iran). He obtained his PhD in food science from Universiti Putra Malaysia in 2012. His PhD thesis dealt with shelf life extension of banana using edible coating conjugated with silver nanoparticles. He joined Sahand University of Technology, Iran in 2012 and is currently working as an associate professor in the Faculty of Chemical Engineering. He is the head of the food research institute. His fields of interest include nanobiotechnology, food biotechnology, green processes, and organic and inorganic nanoparticles synthesis.

Javad Rahbar-Shahrouzi

Javad Rahbar-Shahrouzi received his BSc and MSc degrees in chemical engineering from Petroleum University of Technology (2001) and Sharif University of Technology (2004), respectively. He obtained his PhD degree from University of Paris in process engineering (2010). He has been working as an academic staff at Sahand University of Technology since 2011. He is currently vice dean of the Chemical Engineering Faculty. His areas of interest are nanosensor developement as well as modeling, simulation, and process optimization.